

# **Application of low-coherence interferometry to multiplexing of fiber-optic sensors based on highly birefringent fibers**

WACŁAW URBANČZYK

Institute of Physics, Wrocław University of Technology, Wybrzeże Wyspiańskiego 27, 50–370 Wrocław, Poland.

WOJTEK J. BOCK

Laboratoire d' Optoélectronique, Département d'Informatique, Université du Québec à Hull, P.O. Box 1250, Station B, Hull, Québec J8X 3X7, Canada.

MACIEJ WITCZYŃSKI

Institute of Physics, Wrocław University of Technology, Wybrzeże Wyspiańskiego 27, 50–370 Wrocław, Poland.

Results of experimental studies on coherence multiplexing of a greater number of sensors based on highly birefringent fibers are presented. We propose a flexible detection system based on a Wollstone prism which allows demultiplexing of several serially connected pressure and temperature sensors. The proposed method of multiplexing is simple, inexpensive, and assures absolute accuracy of each multiplexed sensor about 0.5% of the full scale.

## **1. Introduction**

There is a well documented need, especially in civil engineering, for fiber-optic sensors which are inherently immune to EMI, more sensitive, cheaper and directly compatible with increasingly popular fiber-optic transmission and telemetry systems. For effective performance monitoring of a structure, a large number of simultaneously working fiber-optic sensors must be placed in its strategic locations.

There are many papers published on coherence multiplexing of fiber-optic sensors. Theoretical analysis [1]–[6] indicates the possibility of multiplexing dozens of fiber-optic sensors but in practically realized systems the number of multiplexed sensors most often equals two [7]–[9]. There are many factors limiting the maximum number of multiplexed sensors. One of them is the phenomenon of degradation of the contrast of white-light interference patterns with increased number of multiplexed sensors. Other problems arising in complex coherence-multiplexed systems are the power budget and the necessity to properly choose and precisely control optical group imbalances of all sensors in the system in order to finally achieve separation of the signal and noise interference patterns.

In many practical applications it is necessary that all multiplexed sensors be temperature-compensated. However, the requirement of temperature-compensation is in contradiction with the principle of the coherence multiplexing, which requires significantly different group imbalances between all multiplexed sensors. Eliminating this contradiction is the necessary condition to multiplex a greater number of temperature-compensated sensors.

In this paper, we present the way of overcoming most of the difficulties listed above for fiber-optic sensors based on highly birefringent fibers. Such sensors are easy to manufacture, especially that the group imbalance may be controlled by measuring the length of all sensor's elements.

## 2. Detection method

Performance of interferometric sensors depends very much upon their configuration and detection techniques applied. In contrast to classical bulk interferometers, using highly coherent light leads to significant noise increase in fiber-optic interferometric devices. This happens because all scattered light and beams reflected back at splices and connectors (noise beams) finally reach the detector and produce their own noise interference signals. As the propagation constant of the fundamental mode in single-mode fibers is sensitive to environmental parameters, such as temperature, elongation and bending, the phase shifts between noise beams fluctuate in time, which results in an unpredictable intensity variation overlapping with response of the interferometric sensor. In classical bulk interferometers this phenomenon is practically not observed because most of the back-reflected beams are blocked by spatial filters and, furthermore, the phases of the noise beams are much less sensitive to environmental parameters because they propagate in the air.

Due to coherent noise, the resolution of fiber-optic interferometric sensors employing highly coherent light and direct intensity measurement is low and typically does not exceed  $\lambda/50$ . The fringe counting method is frequently used in such sensors. The resolution of this detection technique is also low (typically  $\lambda/4$ ) and, furthermore, it allows no absolute measurements of the phase shift. To overcome the problem of coherent noise and the unambiguity of measurements, two detection methods based on low coherent light have been developed. These are low coherence interferometry (also known as a white-light interferometry) with direct phase recovery or spectral decoding. In white-light interferometric systems, the noise beams reaching the detectors cannot interfere because their optical path delays differ much more than the coherence length of the source. This results in a coherent noise decrease by a few orders of magnitude compared to coherent systems.

White-light interferometric systems with direct phase recovery are usually composed of sensing and decoding interferometers arranged in tandem [10]. The optical path delays introduced by the two interferometers have to match each other and be greater than the coherence length of the source. If these two conditions are fulfilled the differential white-light interference pattern can be observed at the output of the decoding interferometer. This pattern is used to directly recover the phase

shifts or group delays (depending on the detection method) induced in the sensing interferometer, which can be located at a large distance from the decoding interferometer.

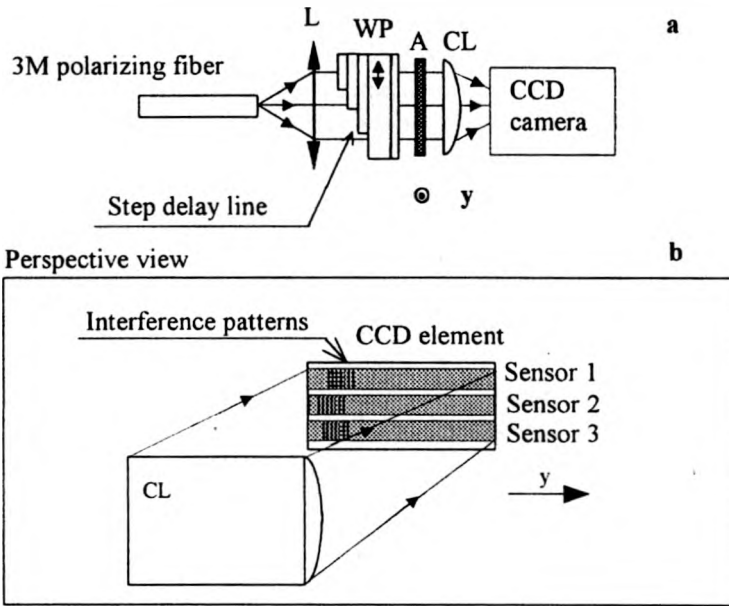


Fig. 1. Scheme of a decoding interferometer (a) and locations of the white-light interference patterns on the CCD array (b).

The detection system we developed to decode simultaneously several sensors based on HB fibers is shown in Fig. 1. The total optical group delay introduced by each sensor has to be greater than the coherence length of the source and different from group delays introduced by other sensors. Essential part of the decoding interferometer is a Wollaston prism made of crystalline quartz. The polarization axes at the end of 3M polarizing fiber connecting sensors with the decoding interferometer are aligned at  $45^\circ$  with respect to polarization axes of the Wollaston prism. Therefore, the linearly polarized output beam emerging from the end of 3M fiber is divided by the Wollaston prism into two orthogonally polarized, slightly divergent beams which may interfere after passing the analyzer. The interference pattern is registered by the CCD camera with the resolution of 1300 pixels in horizontal direction. Cylindrical lens is used to improve the illumination of the CCD array. In front of the Wollaston prism the step delay line, composed of calcite and crystalline quartz plates, is placed. In this way the CCD array is divided into several scanning strips, each of them serving for detection of respective sensor. The total thickness of retardation plates are chosen such that at zero pressure applied to the sensors, the white-light interference patterns arise near the left edges of the scanning areas, as shown in Fig. 1b. It is well known [11] that hydrostatic pressure increases modal

birefringence of HB fibers. On the other hand, the Wollaston prism introduces a group retardation which increases linearly from its left to right edge. Therefore, application of higher pressure to the sensing fibers results in the shifts of the white-light interference patterns towards the right edges of the scanning areas. This is because the center of the white-light interference pattern is always located at this place on the CCD array, at which the group delay introduced by the sensor is compensated by the sum of group delays introduced by the delay line and the Wollaston prism. For each pressure sensor the displacement  $\Delta y$  of the white-light interference pattern is proportional to pressure changes and may be expressed by the following equation:

$$\Delta y = qL_s \frac{\partial \Delta N_s}{\partial P} \Delta P \quad (1)$$

where  $q$  is a proportionality coefficient related to the geometry of the receiving interferometer, and  $\partial \Delta N_s / \partial P$  is sensitivity of the group modal birefringence to hydrostatic pressure or temperature, and  $L_s$  is the length of the sensing fiber. The same equation describes response of temperature sensors.

The processing performed on a signal digitized by the CCD camera should therefore establish the centre of the white-light interference pattern. The details of the processing method are described elsewhere [12]. Using this method it is possible to determine the centre of the white-light interference pattern with the resolution of 4 pixels which assures the relative resolution of the detection unit up to about 0.5% of the full scale. Note that the detection method applied enables absolute measurement of hydrostatic pressure or temperature, with no initialization problems. Furthermore, the method is to a high degree insensitive to intensity fluctuations of the source because only the position of the interference pattern is determined.

### 3. Serially multiplexed systems

One of the most important problems to be solved in fiber-optic measuring devices is temperature compensation. In sensors based on highly birefringent fibers, the configuration first proposed by WADE and DAKIN [13] is usually applied to achieve this goal. In this configuration the sensing interferometer is composed of two lengths of HB fiber spliced together with polarization axes rotated by  $90^\circ$  which assures compensation of phase shifts induced simultaneously in both fibers. As only one of the two fibers constituting the sensor is subjected to the measurand changes, a measurand-induced phase shift remains uncompensated. On the other hand, both fibers are exposed to identical temperature changes which assures temperature desensitization of the sensor. Therefore, perfect temperature compensation for the sensor (neglecting second-order effects [14], [15]) may be achieved when the cross-spliced HB fibers are precisely equal, which means that the total group imbalance of the sensor is always equal to zero. This is in serious contradiction with the principle of coherence multiplexing where every sensor in the system has to have a specific group imbalance enabling its read-out by the receiving interferometer.

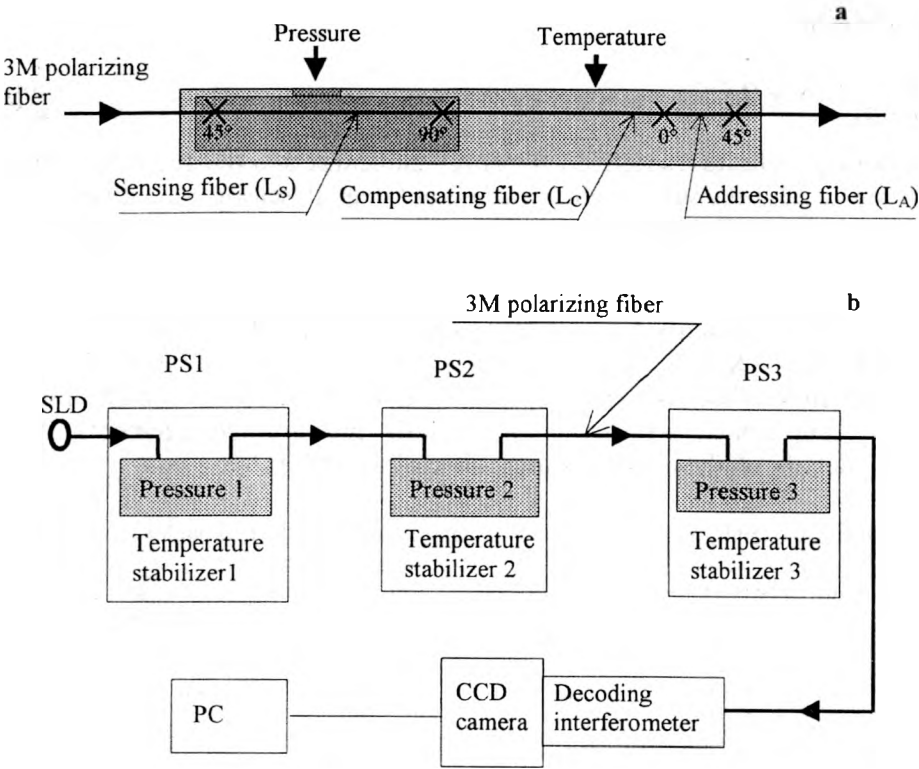


Fig. 2 Details of a temperature compensating configuration (a) and scheme of three serially connected pressure sensors (b).

We propose a new configuration for temperature compensation in order to achieve simultaneously both temperature compensation and possibility of addressing. In this configuration every sensor in the system is composed of three elements: sensing, addressing, and compensating fibers. The sensing and compensating fibers are spliced together with polarization axes rotated by  $90^\circ$  while the compensating and addressing fibers with polarization axes aligned at  $0^\circ$ , as shown in Fig. 2a. The lengths of the compensating ( $L_C$ ) and the addressing fibers ( $L_A$ ) are adjusted in such a way that their overall phase response to temperature is balanced by the response of the sensing fiber ( $L_S$ ) according to the following equation:

$$K_S^T L_S - K_A^T L_A - K_C^T L_C = 0 \tag{2}$$

where:  $K_S^T$ ,  $K_A^T$ ,  $K_C^T$  are temperature sensitivities. The total group imbalance  $\Delta R$  between polarization modes at the output of such a sensor is given by the equation

$$\Delta R = \Delta N_S L_S - \Delta N_A L_A - \Delta N_C L_C \tag{3}$$

where  $\Delta N_S$ ,  $\Delta N_A$ ,  $\Delta N_C$  are modal group birefringences of respective fibers. In order to avoid overlapping of the noise and the signal interference patterns, the total group imbalance of every additional sensor connected to the serial system has to satisfy the

following condition:

$$\Delta R_k = \sum_{i=1}^{k-1} (\Delta R_i + Q_i) \quad (4)$$

where  $\Delta R_i$  and  $Q_i$  indicate respectively the group imbalance and the operation range of the  $i$ -th sensor, and the summation is carried out over all sensors already existing in the system. To simplify the construction of the sensors we used two types of HB fiber: Fibercore HB 800 for compensating and sensing elements, and Corning HB 800 for the addressing element. These fibers have very similar modal group birefringence and significantly different sensitivities to temperature which are equal to  $\Delta N = 604 \times 10^{-6}$ ,  $K^T = 0.54$  rad/Km for Corning HB and  $\Delta N = 568 \times 10^{-6}$ ,  $K^T = 4.8$  rad/Km for Fibercore HB, respectively. Using these fibers we built several temperature compensated sensors for hydrostatic pressure measurements. The construction details of these sensors are collected in the Table.

T a b l e. Elements and total group imbalances of all sensors used in coherence multiplexed systems

Name of the sensor and its operation range	Sensing fiber	Compensating fiber	Addressing fiber	Total group imbalance
Pressure sensor PS1 range 0–30 MPa	Corning PMF-38 $L_S = 16.30$ m	Corning HB 800 $L_C = 16.25$ m	—	$45\lambda$
Pressure sensor PS2 range 0–30 MPa	Corning HB 800 $L_S = 16.90$ m	Corning HB 800 $L_C = 16.25$ m	Fibercore HB 800 $L_A = 0.32$ m	$380\lambda$
Pressure sensor PS3 range 0–30 MPa	Fibercore HB 600 $L_S = 2.84$ m	Corning HB 800 $L_C = 3.27$ m	Fibercore HB 600 $L_A = 1.04$ m	$1600\lambda$
Temperature sensor TS1 range (–50)–(+50) °C	Fibercore HB600 $L_S = 3.20$ m	—	—	$1500\lambda$
Temperature sensor TS2 range (–50)–(+50) °C	Corning HB 800 $L_S = 5.20$ m	—	—	$4700\lambda$

As the temperature sensors we used single elements of HB fibers spliced to the linking fibers with polarization axes rotated by  $45^\circ$ . The sensing as well as the compensating and addressing fibers of the pressure sensor were wound in coils and mounted in two compartments of the specially designed sensor housing. The temperature sensor and the 3M polarizing fiber used as a link may also be coiled and mounted together with the compensating and addressing elements of the pressure

sensor. In this way, it is possible to incorporate two sensors for measuring different parameters in one sensor head. Another possibility is to locate pressure and temperature sensors at distant places.

The system is powered by a superluminescent diode with 1 mW output power and coherence length of about 15  $\mu\text{m}$  ( $\lambda_0 = 820 \text{ nm}$ ). The source, all sensors, and the receiving interferometer are connected with 3M polarizing fiber. Such a configuration benefits in maximum contrasts of interference patterns (equal to 0.5) associated with all sensors in the system and these contrasts do not depend on the number of multiplexed sensors [4].

We built and tested two configurations of serially multiplexed systems. The first system presented in this paper was composed of three temperature-compensated pressure sensors, while in the second configuration two temperature-compensated pressure sensors and two temperature sensors were serially multiplexed.

### 3.1. Three temperature-compensated pressure sensors

This system consisted of three serial temperature-compensated pressure sensors PS1, PS2, and PS3 (Fig. 2b). As there are 8 independent interferometers in such a system, their group retardations have to be carefully controlled in order to avoid overlapping of the signal and cross-interference patterns. Locations of the noise and signal patterns for every sensor in the system are shown in Fig. 3. For sensor PS1, the two signal patterns positioned at  $\pm 45\lambda$  slightly overlap with the central pattern produced by the receiving interferometer. The sensor's initial group imbalance (at atmospheric pressure) equal to  $45\lambda$  is, however, large enough to determine the center of signal pattern with precision of one half of interference fringe. For sensors PS2 and PS3 the signal patterns are located between the two noise patterns corresponding respectively to the cross-interference  $\text{PS2} \pm \text{PS1}$  and  $\text{PS3} \pm \text{PS1}$ , which are observed with lower contrast. The minimum distance (equal  $45\lambda$ ) between the signal and noise patterns is observed again when sensor PS1 is at atmospheric pressure.

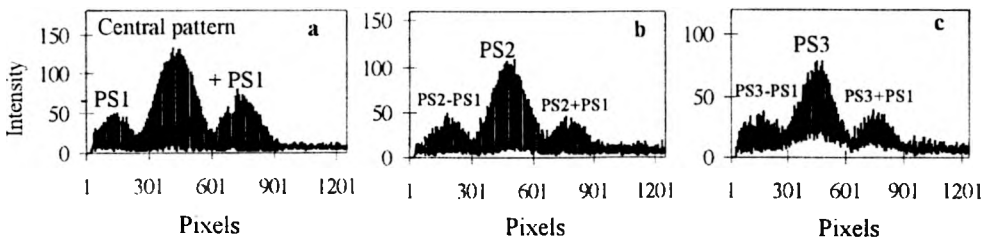


Fig. 3. Locations of signal and noise interference patterns for sensor PS1 (a), PS2 (b) and PS3 (c). Slowly varying bias intensity was filtered out by a special numerical procedure.

The compartment of the sensor head containing the sensing fiber was connected to Harwood DWT-35 Deadweight Tester which delivered the desired pressure with at least 0.1% accuracy. The sensor housings were immersed in a temperature stabilized oil bath to allow for temperature stabilization with the precision of 0.1  $^{\circ}\text{C}$ . The pressure characteristics for each sensor were measured at 5  $^{\circ}\text{C}$ , 25  $^{\circ}\text{C}$  and 45  $^{\circ}\text{C}$ .

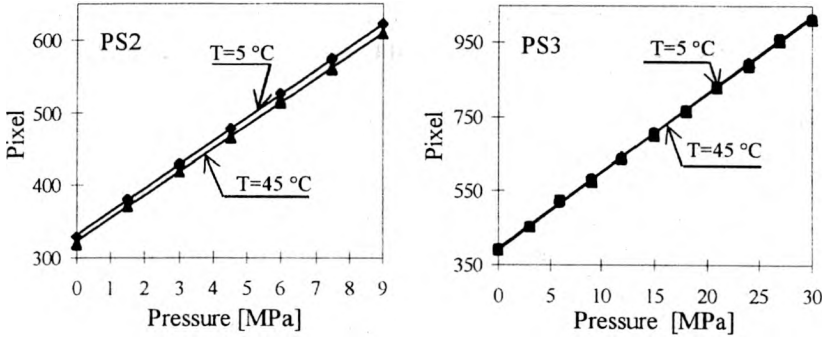


Fig. 4. Pressure characteristics measured at  $T = 5\text{ }^{\circ}\text{C}$  and  $T = 45\text{ }^{\circ}\text{C}$  for the sensor with highest (PS2) and lowest (PS3) temperature drift.

to determine the temperature drifts (see Fig. 4). They were equal to 3%, 10% and 1% of the full scale per  $40\text{ }^{\circ}\text{C}$ , for sensors PS1, PS2 and PS3, respectively. Only compensation of sensor PS3 was close to perfect and its temperature drift was practically limited by the second-order effects. This system configuration may be useful for hydrostatic pressure measurements in which medium temperature stability is required.

**3.2. Two temperature-compensated pressure sensors and two temperature sensors**

In this case the system was composed of four sensors: PS1, PS2, TS1, TS2 (Fig. 5). Such a system can be used either for independent monitoring of pressures and temperatures at four different points or for temperature desensitization of the two pressure sensors. In the configuration tested, temperature sensors TS1 and TS2 were installed in housings of pressure sensors PS1 and PS2, respectively. This provided the possibility of temperature-correction of pressure readings for sensors PS1 and PS2 by on-line processing of measurement data delivered simultaneously from PS1 and TS1 as well as PS2 and TS2. With the correction method described in [16] the residual temperature drift of the pressure sensor PS2, initially reaching 0.25% of the full scale per  $^{\circ}\text{C}$ , was reduced to 0.02% per  $^{\circ}\text{C}$ . Such a system may be used for precise measurements of quasi-static pressures in a wide temperature range.

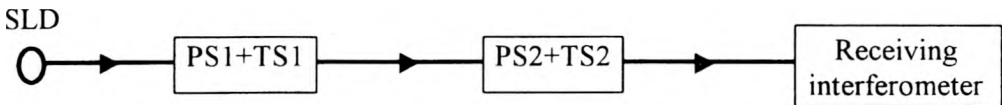


Fig. 5. Two temperature compensated pressure sensors and two temperature sensors in serial configuration.

Simultaneous responses of all multiplexed sensors to stepping type increases of pressures and temperatures are shown in Fig. 6. We observed a drop of the sensor resolution to 1% of the full scale which was associated with too small power at the output of the system (20 nW).

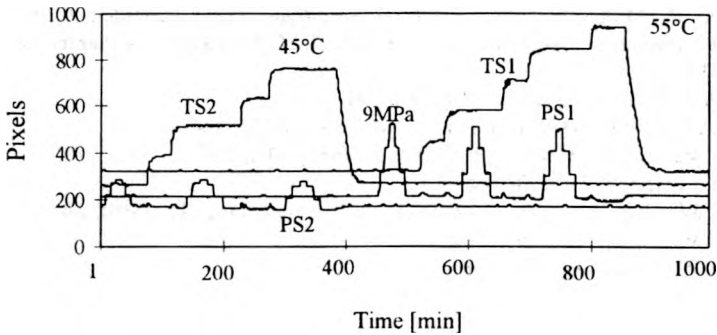


Fig. 6. Simultaneous responses of multiplexed sensors: TS1, TS2, PS1, PS2 for step type increase of pressure and temperature:  $T_1 = 5^\circ\text{C}, 15^\circ\text{C}, 25^\circ\text{C}, 35^\circ\text{C}, 45^\circ\text{C}, 55^\circ\text{C}$ ;  $T_2 = 5^\circ\text{C}, 15^\circ\text{C}, 25^\circ\text{C}, 35^\circ\text{C}, 45^\circ\text{C}$ ;  $P_1 = 0.1\text{ MPa}, 3\text{ MPa}, 6\text{ MPa}, 9\text{ MPa}$ ;  $P_2 = 0.1\text{ MPa}, 1.5\text{ MPa}, 3\text{ MPa}, 3.6\text{ MPa}$ .

#### 4. Conclusions

We proposed and tested a new configuration for a system of coherence multiplexed sensors based on highly birefringent fibers. In this system every pressure sensor is temperature compensated while keeping its individual group imbalance necessary for coherence addressing. This feature was achieved by employing a modified temperature compensation scheme in which every sensor was composed of three elements: sensing, compensating and addressing fibers. Furthermore, we used 3M polarizing fiber as a linking between successive sensors assuring maximum contrast (equal to 0.5) for all signal interference patterns which in addition does not depend on the number of sensors in the system. This is an important advantage over the system with HB type linking fibers where the contrast degradation is observed with increasing number of multiplexed sensors.

The maximum number of sensors in the serial system is limited by the power budget and not more than four sensors may be multiplexed in this way. To further increase the number of multiplexed sensors, a mixed serial-parallel configuration should be applied.

#### References

- [1] BROOKS J. L., WENTWORTH R. H., YOUNGQUIST R. C., TUR M., KIM B. Y., SHOW H. J., *J. Lightwave Technol.* **3** (1985), 1062.
- [2] BLOTEKJAER K., WENTWORTH R. H., SHAW H. J., *J. Lightwave Technol.* **5** (1987), 229.
- [3] WENTWORTH R. H., *J. Lightwave Technol.* **7** (1989), 941.
- [4] URBAŃCZYK W., BOCK W. J., *Opt. Eng.* **32** (1993), 2100.
- [5] URBAŃCZYK U., KURZYŃOWSKI P., WOŹNIAK A. W., BOCK W. J., *Opt. Commun.* **135** (1997), 1.
- [6] URBAŃCZYK W., KURZYŃOWSKI P., WOŹNIAK A. W., BOCK W. J., *Optik* **104** (1997), 153.
- [7] GERGES A. S., FARAHI F., NEWSON T. P., JONES J. D. C., JACKSON D. A., *Electron. Lett.* **23** (1987), 1110.
- [8] FARAHI F., NEWSON T. P., JONES J. D. C., JACKSON D. A., *Opt. Commun.* **65** (1987), 319.

- [9] GUSMEROLI V., VAVASSORI P., MARTINELLI M., *A coherence-multiplexed quasi-distributed polarimetric sensor suitable for structural monitoring*, Proc. 6th Int. Conf. OFS'89, Paris, September 18–20, 1989, pp. 513–518.
- [10] RAO Y. J., JACKSON D. A., Meas. Sci. Technol. **7** (1996), 981.
- [11] BOCK W. J., DOMAŃSKI A. W., WOLIŃSKI T. R., Appl. Opt. **29** (1990), 3484.
- [12] BOCK W. J., URBAŃCZYK W., ZAREMBA M., Opt. Commun. **101** (1993), 157.
- [13] DAKIN J. P., WADE C. A., Electron. Lett. **20** (1984), 51.
- [14] BOCK W. J., URBAŃCZYK W., BUCZYŃSKI R., DOMAŃSKI A. W., Appl. Opt. **33** (1994), 6078.
- [15] BOCK W. J., URBAŃCZYK W., Appl. Opt. **35** (1996), 6267.
- [16] BOCK W. J., URBAŃCZYK W., Appl. Opt. **37** (1998), 3897.

*Received November 18, 1998  
in revised form February 10, 1999*